Theory of point defects in GaN, AlN, and BN: Relaxation and pressure effects

I. Gorczyca,* A. Svane, and N. E. Christensen
Institute of Physics and Astronomy, University of Aarhus, DK-8000 Aarhus C, Denmark
(Received 11 January 1999)

Native defects and some common dopants in cubic GaN, AlN, and BN are examined by means of *ab initio* calculations using a supercell approach in connection with the full potential linear muffin-tin orbital method. The atomic positions, the electronic structure, and the defect formation energies are calculated. In particular, the vacancies are calculated to be abundant defects. The high-pressure behavior of the defect states is also studied, and it is found that the pressure coefficients of the defect states depend mainly on their position in the energy gap. [S0163-1829(99)02731-9]

I. INTRODUCTION

Although less studied in the past than other III-V compounds, nitrides now belong to a rapidly growing field of solid-state research. III-V nitrides exhibit some unique properties, such as a large band gap, strong interatomic bonds, and a high thermal conductivity, which make them ideal materials for optoelectronic and high-temperature/high-power devices. The recent rapid increase in research on nitrides has been stimulated by the successful fabrication of bright, highly efficient GaN-based green-blue light-emitting diodes.

Since the electronic quality of a semiconductor is largely determined by the nature and number of its native defects and impurities, it is important to understand their properties. Despite their importance for device applications, too little is still known about intrinsic defects in the III nitrides. The experimental investigations in this field[1] are accompanied by first-principles calculations of both native defects and dopants (such as C, Si, Ge, Be, Zn, Mg, O, and H) (see, for example, Refs. 2–5) and their complexes (such as Mg-H, V-H, V-V, and V-O) (see, for example, Refs. 6–8) in nitrides and nitride-based alloys and heterostructures. Calculations of total energies and electronic structures of defects make it possible to investigate the character and position of defect levels, their atomic structure, and the formation energy.

The aim of the present paper is to present results of calculations of electronic structures of some point defects for the most interesting nitrides: (i) GaN, which is most advanced in research and technology; (ii) AlN, less used, but similar to GaN and often used in applications in heterostructures $Al_xGa_{1-x}N$/GaN (e.g., in field effect transistors); and (iii) BN, which in particular is interesting due to its extreme hardness (similar to that of diamond). In our study we focus on the similarities and differences in defect properties between these compounds by calculating the electronic structures, the defect formation energies, and the high-pressure behavior of the defect states. In particular, the pressure analysis is interesting because a comparison of experimentally obtained pressure dependence of the defect levels with theoretical results can be a very useful tool in identification and characterization of the defect states.

We study vacancies, antisites, and substitutional impurities such as C, Zn, and Mg in GaN and AlN, and C in BN. The choice of impurities to be studied is motivated by their frequent usage as dopants of III-V semiconductors. Further, both C and Mg may be unintentionally incorporated as contaminants during the growth of GaN and AlN crystals.

Native point defects are known to play an important role in GaN. In GaN, *n*-type as well as *p*-type doping has been achieved. Nitrogen vacancies were long suspected to be the source of *n*-type conductivity. Recently, however, unintentional contamination has been shown to be the source of the dominant donors. Nonetheless, nitrogen vacancies still act as compensating centers in *p*-type GaN. Ga vacancies are deep acceptors and as such are more likely to occur in *n*-type material. They have been associated with compensation of highly doped *n*-type GaN and proposed to be the source of the commonly observed ''yellow luminescence.'' Other types of point defects (antisites or interstitials) have sometimes been invoked to explain experiments. First-principles calculations of formation energies have shown, however, that their formation energies are high, and therefore, they are unlikely to form in appreciable concentrations during GaN growth.

AlN has so far resisted any doping attempts, either *n* or *p* type. This may be due to its very wide band gap (6.1 eV), or it may be due to the presence of many native defects.

BN is one of the most interesting III-V compounds, both from theoretical and practical points of view. Physical properties such as extreme hardness, high melting point and interesting dielectric, thermal, and optical characteristics are very promising for applications in electronics, optoelectronics, and coating. Bulk BN shows a polymorphism similar to carbon, crystallizing in a hexagonal (graphite-like) and a zinc-blende structure; cubic BN resembles diamond in hardness. BN exists also in the wurtzite structure. The cubic BN was synthesized in 1957 (Ref. 9) and has an indirect gap $E_g = 6.4$ eV.[10]

The paper is organized as follows. In the next section we describe the methods used in the calculations. In Sec. III, we present the results of the supercell calculations comparing them with those obtained previously by the Green's function (GF) linear muffin-tin orbital[11] (LMTO) method and with other theoretical and experimental results. We discuss the effects of lattice relaxation near the defects and their influence on the defect level positions in the energy gap. Also the pressure effects are described in Sec. III. The defect formation energies are presented in Sec. IV, and the last section contains summary and conclusions.

 ©1999 The American Physical Society

II. METHODS

In a previous paper[11] we reported the results of the electronic structure calculations of native defects and impurities in GaN and AlN obtained by the GF technique[12] in the frame of the LMTO method[13] in the atomic sphere approximation (ASA). The GF LMTO method allows us to study different charge states of defects represented by single energy levels, but only *ideal* substitutional defects can be treated by our implementation of this method. The GF LMTO method gives a fast way to get both neutral and charged states of defects and to derive pressure coefficients (or deformation potentials) for the impurity levels. But, the assumption that the host atoms remain in their ideal positions can lead to substantial errors in the level energies in cases with pronounced relaxations, and therefore, we use here the supercell method to examine such effects.

Relaxations cannot be predicted from total-energy calculations using the ASA version of LMTO. The full nonspherical shapes of potentials and charge distributions must be taken into account. We do this by combining the supercell approach with the full potential (FP) version[14] of the LMTO scheme. In contrast to the GF LMTO method where defect states are characterized by a single energy level, in the supercell approach, large but finite cells, each containing a defect, are repeated *ad infinitum*, leading to impurity bands with finite widths. In this case, we estimate the impurity levels in the band gap as the center of gravity of the impurity band.

Calculations are performed using 32-atom supercells. We choose all (nonoverlapping) muffin-tin spheres to have the same size. As usual, in open structures, empty spheres (of the same size as the atomic ones) are inserted in the interstitial regions to improve the packing fraction. (In the FP LMTO these are only used to enhance the accuracy of the interstitial integrals and charge density.) In the calculations we have used a basis set that includes partial waves of s, p, and d character on each atomic site, with a total of 44 LMTO orbitals per formula unit. The **k**-space integrations used 216 **k** points in the Brillouin zone, and convergence tests were made with 512 **k** points.

The local-density approximation (LDA) (Ref. 15) to the density functional theory is used, by which exchange and correlation effects are accounted for by a simple local potential. The fundamental gaps derived from the LDA band structures are generally 50–100 % too small. This has consequences for defect calculations, in particular for the energy-level positions of bound states in the gap. To overcome this problem in the GF LMTO method, we have chosen to rigidly shift the conduction bands upward to match the experimental minimum gap (the ''scissors operator'').

BN crystallizes usually in the cubic phase, whereas GaN and AlN can crystallize in two phases, the cubic (zinc blende) and hexagonal (wurtzite) phases. We study here the cubic phase, believing that there is little difference in impurity level positions of the two phases. This is supported by the comparison of defects in hexagonal and cubic GaN made by Neugebauer and Van de Walle,[16] who found only minor differences in formation energy and atomic relaxations between these two hosts. Further, the energy-level positions were practically the same. The most distinct difference is a small splitting of the t_2 gap states related to the lower symmetry of the wurtzite structure compared to the cubic structure.

III. DEFECT LEVEL POSITIONS; RELAXATION AND PRESSURE EFFECTS

We consider the cation and anion vacancies and antisites, a substitutional carbon impurity on the cation, as well as on the anion site, and in GaN and AlN also Zn and Mg on the cation site. In Tables I–III the charge-state specifications, energy-level positions, and (in parentheses) their pressure coefficients, as calculated by both the supercell and the GF methods are given for all the considered defects in GaN (Table I), in AlN (Table II), and in BN (Table III). The value of the relaxation (R) is given in percent of the bond length, positive R means that the bond distance between defect and the nearest neighbors increases.

The supercell calculations, combined with the full potential LMTO, are performed for two cases: without and with the lattice relaxation effects included. For all cases except the nitrogen antisite in GaN and AlN, the relaxation is symmetrical, i.e., the atoms surrounding the defect are moved outward or inward symmetrically. The case of the nitrogen antisite will be discussed below in detail.

Performing the supercell calculations, we concentrate in the present work on neutral charge states only. From the GF method we get information about neutral as well as charged states, but without lattice relaxation.

The energy gap of AlN is assumed to be 6.1 eV (experimental value for wurtzite structure), almost twice that of GaN (3.25 eV). The experimental energy gap of BN is 6.4 eV. In the GF calculations, the conduction bands are rigidly upshifted to reproduce these experimental gaps.

In GaN the calculated pressure coefficient of the main energy gap is 38 meV/GPa, close to the 40 meV/GPa found earlier by the ASA LMTO.[17] Cubic AlN has an indirect energy gap (Γ-X) with the pressure coefficient 1.9 meV/GPa (ASA LMTO: 1.7 meV/GPa), whereas the pressure coefficient at the Γ point is 43 meV/GPa (ASA LMTO: 42 meV/GPa).

The fundamental gap is also in BN indirect (Γ-X) with the pressure coefficient 3.0 meV/GPa (ASA LMTO: 2.8 meV/GPa), whereas the pressure coefficient at the Γ point is 14 meV/GPa (ASA LMTO: 13 meV/GPa).

A. Vacancies

A cation (Ga, Al, or B) vacancy in the neutral charge state is a triple acceptor with a level close to the valence-band maximum (VBM), which can be filled with three more electrons, introducing a set of levels above the valence-band edge. These acceptor states lie in all the nitrides considered here between 0.2 eV and 2.4 eV above the VBM.

In GaN the neutral state of V_{Ga} is lying around 0.2 eV above the VBM, according to both the supercell and the GF approach. The lattice relaxation only slightly affects this state. This agrees very well with the results of pseudopotential calculations for the wurtzite structure made by Boguslawski *et al.*[18] using quantum molecular dynamics (0.3 eV)

TABLE I. The charge state specifications, the relaxation (R) in percent of the bond length, (positive R means that the bond distance between defect and the nearest neighbors increases), energy level positions (in eV), and, in parentheses, their pressure coefficients (in meV/GPa) as calculated by both the supercell and the GF method for defects in GaN.

Method		''Supercell''		''GF''			
	R	E dE/dP	E dE/dP	E dE/dP	E dE/dP	E dE/dP	E dE/dP
GaN:V_{Ga}		●●●○○○		●●●○○○	●●●●○○	●●●●●○	●●●●●●
	0	0.2		0.2	0.4	0.75	1.1
		(−1.2)		(−1.5)	(−1.8)	(−1.5)	(0.1)
		0.25					
	8	(−0.8)					
GaN:V_N		●●	●○○○○○	●●	●○○○○○		
	0	$E_V-0.1$	$E_C+0.5$	v.b.	c.b.		
		(−3)	(16)		(15)		
		$E_V-0.1$	$E_C+0.5$				
	−2	(−3)	(16)				
GaN:Ga_N		●●●●○○		●●●●○○	●●●●●○	●●●●●●	
	0	1.2		0.7	0.9	1.3	
		(8)		(5)	(6)	(7)	
	12	2.0					
		(10)					
GaN:N_{Ga}		●●	○○○○○○	●○	●●	○○○○○○	
	0	0.55	2.4	0.14	0.74	2.0	
		(7)	(15)	(3.8)	(7.3)	(23)	
	−30	0.8	2.2				
	−7	(9)	(14)				
GaN:C_{Ga}		●●		●○			
	0	$E_C-0.9$		c.b.			
		(19)					
	−18	$E_C-0.2$					
		(20)					
GaN:C_N		●●●●●○		●●●●●○	●●●●●●		
	0	0.4		0.1	0.5		
		(4)					
GaN:Zn_{Ga}		●●●●●○		●●●●●○	●●●●●●		
	0	0.25		0.1	0.2		
				(0.6)			
	2	0.3					
		(3)					
GaN:Mg_{Ga}		●●●●●○		●●●●●○	●●●●●●		
	0	0.1		v.b.	0.1		
	4	0.15					
		(2)					

and with the pseudopotential calculations by Neugebauer and Van de Walle.[16] Charged states are situated higher in the band gap, in the range 0.4 to 1.1 eV, according to our GF calculations.

In AlN, V_{Al} lies 0.5 eV above the VBM, in agreement with the calculations by Boguslawski *et al.*[18] for the wurtzite structure (0.4 eV). According to the GF calculations, the neutral V_{Al} level is found at 0.6 eV, while charged states are found between 0.9 and 1.9 eV.

The GF calculation predicts that the boron vacancy V_B gives rise to several acceptor states in the range 0.6 eV to 2.4 eV above the VBM. The neutral state, as calculated by the supercell method with the lattice relaxation included, is lying slightly higher (0.9 eV) than the level position obtained without relaxations included by the GF method (0.6 eV) or by the supercell approach (0.7 eV).

Outward, symmetrical, relaxation is found for cation vacancies. In GaN the nearest neighbors are shifted away by

TABLE II. The charge state specifications, the relaxation, energy-level positions (in eV), and their pressure coefficients as calculated by both the supercell and the GF method for defects in AlN. Nomenclature as in Table I.

Method		''Supercell''		''GF''			
	R	E dE/dP	E dE/dP	E dE/dP	E dE/dP	E dE/dP	E dE/dP
AlN:V_{Al}		●●●○○○		●●●○○○	●●●●○○	●●●●●○	●●●●●●
	0	0.4		0.6	0.9	1.5	1.9
		(−0.1)		(2.0)	(2.3)	(2.6)	(3.0)
	11	0.5					
		(0.1)					
AlN:V_N		●●	●○○○○○	●○	●●	●○○○○○	
	0	0.5	$E_C+0.2$	0.14	1.0	5.7	
		(−0.7)	(12)	(−1.7)	(0.0)	(15)	
AlN:Al_N		●●●●○○		●●●●○○	●●●●●○	●●●●●●	
	0	1.8		2.4	3.2	3.8	
		(12)		(17)	(17)	(16)	
	18	3.1					
		(14)					
AlN:N_{Al}		●●	○○○○○○	●○	●●	○○○○○○	
	0	1.2	3.2	1.6	2.4	3.0	
		(15)	(17)	(17)	(19)	(17)	
	−29	1.4	2.8				
	−8	(13)	(16)				
AlN:C_{Al}		●○		●○			
	0	$E_C-0.6$		$E_C-1.4$			
		(23)		(33)			
	−16	$E_C+0.3$					
		(25)					
AlN:C_N		●●●●●○		●●●●●○	●●●●●●		
	0	0.5		v.b.	0.1		
		(2)					
	2	0.5					
		(2)					
AlN:Zn_{Al}	0	●●●●●○		●●●●●○	●●●●●●		
		0.1		v.b.	0.1		
	10	0.35					
		(1.0)					
AlN:Mg_{Al}		●●●●●○		●●●●●○	●●●●●●		
	0	0.2		0.15	0.57		
		(0.9)		(0.9)	(2.2)		
	7	0.3					
		(1.1)					

8% of the bond length; in AlN and BN, a little larger shift, 11%, is found. Comparing the relaxation values with other theoretical results, we have excellent agreement with Mattila *et al.*[19] for AlN. Neugebauer and Van de Walle[16] predicted a 4% relaxation around V_{Ga} (in wurtzite GaN).

From both the supercell and GF calculations, the pressure coefficients of the cation vacancy-induced levels (calculated with respect to the top of the valence band) are very small: negative for GaN, close to zero for AlN, and small positive for BN.

While the cation vacancy level positions are very similar in all compounds considered, the nitrogen vacancy behaves somewhat differently. In GaN, as found from both calculations, the a_1 (s-like) state of V_N forms a resonance 0.1 eV below the VBM, whereas the t_2 (p-like) state appears as a resonance in the conduction band. The approximate position of the t_2 resonance at 0.5 eV above the conduction-band minimum (CBM) as found in the present calculation can be compared to the 0.8 eV above the CBM, as obtained for the wurtzite phase.[18]

TABLE III. The charge state specifications, the relaxation, energy-level positions (in eV), and their pressure coefficients as calculated by both the supercell and the GF method for defects in BN. Nomenclature as in Table I.

Method		"Supercell"		"GF"			
	R	E dE/dP	E dE/dP	E dE/dP	E dE/dP	E dE/dP	E dE/dP
BN:V_B		●●●○○○		●●●○○○	●●●●○○	●●●●●○	●●●●●●
	0	0.7		0.6	1.1	1.7	2.4
		(1.0)		(0.0)	(0.1)	(0.5)	(1.3)
	11	0.9					
		(0.8)					
BN:V_N		●●	●○○○○○	●●	●○○○○○		
	0	$E_V-0.1$	4.9	0.25	5.1		
		(−5)	(5)	(−5)	(6)		
	5	0.6	5.3				
		(−4)	(5)				
BN:B_N		●●●●○○		●●●●○○	●●●●●○	●●●●●●	
	0	1.2		0.7	1.3	2.1	
		(−1)		(0.5)	(0.6)	(0.8)	
	6	1.7					
		(0)					
BN:N_B		●●	○○○○○○	●○	●●	○○○○○○	
	0	4.0	5.1	4.5	4.9	5.4	
		(14)	(10)	(18)	(18)	(11)	
	9	2.6	4.3				
		(13)	(10)				
BN:C_B		●○		●○	●●		
	0	5.1		c.b.	c.b.		
		(7)					
	−3	5.3					
		(7)					
BN:C_N		●●●●●○		●●●●●○	●●●●●●		
	0	0.5		0.1	0.2		
		(0.5)		(−0.9)	(−0.8)		

According to the GF LMTO calculations, the V_N levels in AlN are moved into the band gap. The a_1 (s-like) state of V_N lies 1.0 eV above the VBM (E_V), whereas the t_2 (p-like) state is found to be 0.4 eV below the CBM (E_C). In this case, the supercell approach leads to slightly different results: The s state is in the gap ($E_V+0.5$ eV), and the p state is degenerate with the conduction band ($E_C+0.2$ eV).

In BN we find both s- and p-type states of the N vacancy in the energy gap. The GF and supercell calculations yield an a_1 (s-like) state of V_N close to the valence-band edge (at 0.2 eV according to the GF and supercell calculations without relaxations; at 0.6 eV according to the supercell approach with lattice relaxations included), whereas the t_2 (p-like) state appears close to the conduction-band edge (5.1 eV, 4.8 eV, and 5.3 eV, respectively, for the GF and supercell calculations without and with relaxations). In previous calculations of the V_N in the wurtzite phase,[20] the position of the p-like level was found ≈ 1 eV below the CBM. Since the band gap of cubic BN is 6.4 eV, this value compares favorably with the value of ≈ 5 eV above the VBM obtained for the position of the p-like state in the present work.

Lattice relaxations are small near the nitrogen vacancy, in all materials considered. In GaN we find that the nearest-neighbor Ga atoms relax inwards by 2% of the bond length. This is in agreement with the pseudopotential calculations[21] (inward relaxation $\approx 3\%$ of the bond length). The above small relaxation does not change the positions of the energy levels. The relaxations in AlN were found to be vanishingly small.

In BN lattice relaxations near an N vacancy are slightly larger and still symmetrical. We find that the nearest-neighbor boron atoms relax outwards by 5% of the bond length, which leads to small upward shifts of the defect levels.

The calculated pressure coefficients for the nitrogen vacancies are similar in GaN and AlN. They are very small and negative for s-like states and large and positive (around 15 meV/GPa) for p-like states resonant with or just below the

conduction band. In BN the pressure coefficients are also negative for the *s*-like state and positive, but smaller (5 meV/GPa), for the *p*-like state.

B. Antisites

Antisite defects introduce deep levels. Lattice relaxations connected with these defects are very pronounced but quite different for cation and nitrogen antisites. The cation antisite defects, Ga_N, Al_N, and B_N, are in their neutral charge states double acceptors (occupied with four electrons). The Ga_N level is about 2.0 eV above the VBM in GaN according to our supercell calculation. This is a little higher than the position (≈ 1.7 eV) of the same state obtained by the pseudopotential calculations for the wurtzite phase.[18]

In AlN the Al_N energy level is close to the midgap, i.e., ≈ 3 eV above the VBM. In BN, the neutral state of B_N, according to the GF calculations, is about 0.8 eV above the VBM. Negative charge states, B_N^- and B_N^{--}, are lying at 1.3 eV and 2.1 eV.

In all compounds we find an outward relaxation around the cation antisite. In GaN the distance to the nearest neighbors is increased by 12% of the ideal bond length, in AlN by 18%. The result for GaN is in agreement with the pseudopotential calculations[18] (11% outward relaxation). For GaN and AlN we find substantial differences between level positions as calculated by different methods or with and without lattice relaxations. The energy levels obtained by the GF method are lying about 0.5 eV higher (lower) in AlN (GaN) than those obtained by supercell calculations without lattice relaxations. There are large relaxations, and this implies that the energy levels determined by means of our ''nonrelaxed'' calculations differ from those obtained with lattice relaxations included. Indeed, including relaxation effects we observe the upward shift of energy levels of the order of 1 eV (0.8 in GaN, 1.3 in AlN). Relaxed supercell calculations for the same type of defect in BN show that in this case the distance to the nearest neighbors is increased only by 6% of the ideal bond length. But the corresponding neutral state level lies significantly higher (about 1.7 eV above the VBM) than obtained by the supercell method without relaxations included (1.2 eV) and by the GF method (0.7 eV). Thus, the relaxation causes an upward shift of the defect level of the order of 0.5 eV.

The neutral nitrogen antisite defect introduces a doubly occupied a_1 state above the VBM and an empty triplet higher in the band gap. The N antisite defect behaves almost identically in GaN and AlN, and differently in BN. As results from the GF calculations N_{Ga} has an *s*-like state at 0.74 eV above the VBM and an empty *p*-type state at 2.0 eV. Corresponding (i.e., without relaxations) supercell calculations give similar values (0.6 eV and 2.4 eV, respectively). In AlN the empty state is found by the GF method at about 3 eV and similarly by the nonrelaxed supercell method at 3.2 eV, but there is disagreement in the position of the *s*-like state (2.4 eV by the GF and 1.2 eV by the supercell method).

In BN the neutral nitrogen antisite defect N_B introduces a doubly occupied a_1 state in the middle of the band gap and an empty triplet close to the CBM. The GF calculation for N_B yields an *s*-like neutral state 4.9 eV above the VBM and an empty *p*-type state at 5.4 eV. The supercell calculations

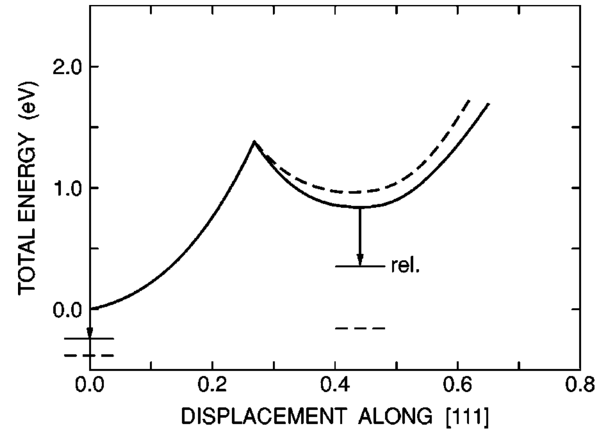

FIG. 1. The total energies for the neutral nitrogen antisite in GaN. Our results are represented by solid lines in comparison with the results by Mattila *et al.* (Ref. 19) (dashed lines). The zero position denotes the ideal geometry, and the displacement along the threefold symmetry axis is measured in units of the nearest-neighbor distance (d_0). The horizontal bars refer to calculations where all the atoms are allowed to relax.

without relaxations give quite similar values, whereas the supercell calculations *with* relaxations give the values about 1 eV lower.

Let us consider lattice relaxations near the N antisite in GaN and AlN. Assuming for the nitrogen antisite the full T_d symmetry, we find a small, 1%, outward displacement of the nearest-neighbor nitrogen atoms. But if we, on the other hand, allow for symmetry changes, we find that the nitrogen antisite distorts strongly along a threefold symmetry axis. In the case of N_{Ga}, the bond distance to the nearest-neighbor atom is reduced by 30% (in agreement with pseudopotential calculations[18]). Supercell calculations for N_{Al} yield a similar result: a reduction of the bond length to the nearest nitrogen atom by 29%, and this agrees with the result obtained by Mattila *et al.*[19] The three remaining neighbors relax inwards by 7% in GaN and by 8% in AlN, but due to the large displacement of the N antisite, the bonds of the three distant neighbors to the antisite N atom are stretched, by 7% in GaN and by 6% in AlN. Note, that the shortest N-N distance (≈ 1.3 Å) in this relaxed structure is closer to the interatomic distance (1.1 Å) in the free N_2 molecule than to the bond length of AlN (1.89 Å) or GaN (1.94 Å).

Taking into account these large relaxations, the changes of the energy-level positions are surprisingly small. The calculated upward shift of *s*-type and downward shift of *p*-type energy levels due to relaxation effects is in the range of 0.2 eV, in both compounds.

We have also investigated the metastability of the nitrogen antisite reported already by Mattila *et al.*[19] When the antisite is displaced along the (111) axis away from the nearest-neighbor atom, a second energy minimum occurs. We find this at a displacement equal to 49% of the bond length for AlN and 45% for GaN. The relaxation of the remaining atoms at the displaced site is axially symmetric—the three atoms surrounding the antisite relax inwards: In AlN by 8% of the bond length, in GaN by 12% of the bond length. The results above are in a good agreement with the pseudopotential calculation by Mattila. *et al.*[19] In Fig. 1 the comparison of our results with those by Mattila *et al.* is

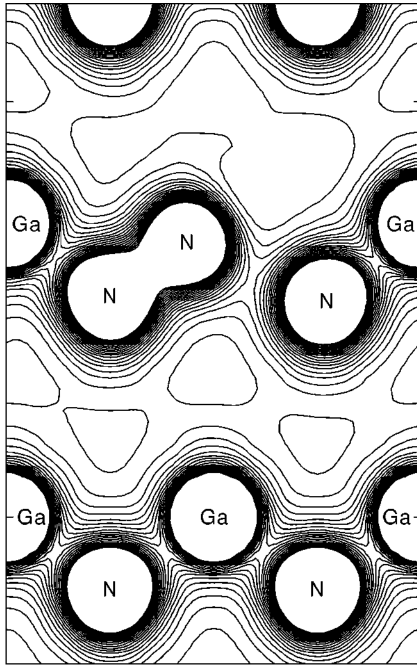

FIG. 2. Contour plot of the valence electron density around the N antisite defect in GaN.

made. The two calculations predict the same stable configuration. The arrows indicate the energy changes due to relaxations. Mattila *et al.*[19] found somewhat larger energy reductions, but the two calculations agree with the undisplaced structure having the lowest energy.

The contour plot in Fig. 2 of the electron density around the N antisite defect in GaN shows the creation of the N_2 ''molecule.'' Contrary to the GaN and AlN cases, there is no distortion of the N antisite symmetry in the case of BN. The outward symmetrical relaxation is found to be about 9% of the bond length. The pressure coefficients of the N antisite levels are in the range of 10–20 meV/GPa for all three nitrides.

C. Dopant levels

In the present work we study the substitutional C, Zn, and Mg impurities in the cases of GaN and AlN, and only carbon in the case of BN. The importance of the C impurity follows from the fact that carbon atoms may be unintentionally incorporated in nitrides during growth. Carbon, as a group-IV atom, is an amphoteric impurity in all compounds considered; so we consider the substitutional carbon on both the cation and the nitrogen site.

The GF calculations show that C_{Ga} introduces a resonant state above the CBM in GaN, whereas supercell calculations give the level position slightly below the CBM. C_{Al} creates in AlN an effective-mass donor level nearly degenerate with the conduction band. According to similar calculations for BN, we find that C_B introduces a state degenerate with the CBM, whereas the supercell calculations give the level position ≈ 1 eV below the CBM (5.3 eV above the VBM). In GaN and AlN, the relaxation around the carbon atom at the cation site is large, and it reduces the nearest-neighbor bond length by $\approx 18\%$ in GaN and $\approx 16\%$ in AlN, in agreement with pseudopotential calculations.[22] The lattice relaxation

TABLE IV. Calculated formation energies, in eV, for native defects and substitutional carbon impurities in BN. Also listed are the chemical potentials of the atoms, likewise in eV. Both B-rich and N-rich growth conditions are considered. The calculated formation energy of bulk BN is 3.9 eV.

	B-rich	N-rich
μ_B	−7.1	−11.0
μ_N	−12.3	−8.3
μ_C	−10.1	−10.1
V_B	8.4	4.5
V_N	4.7	8.6
B_N	4.4	12.3
N_B	13.8	6.0
C_B	7.2	3.3
C_N	1.7	5.6

causes the upward shift of energy levels, both in GaN and in AlN. In BN, on the other hand, the relaxation around the carbon atom is small reducing the nearest-neighbor bond length by $\approx 3\%$, and it changes slightly the position of the impurity level (from 5.2 eV to 5.5 eV above the VBM).

C_N is a shallow acceptor; it introduces several impurity levels, the lowest one (corresponding to the neutral charge state) is located about 0.4 eV above the VBM in GaN, and a little higher, ≈ 0.5 eV, in AlN. The same value is found for C_N in BN according to the supercell calculations. There is no relaxation in the case of C_N in GaN and BN, and there is very small outward relaxation, $\approx 2\%$, in AlN. The results for GaN and AlN are close to those obtained by pseudopotential method,[22] where small inward relaxation is found for GaN (2% of the bond length), with the level position at 0.2 eV, and small outward relaxation for AlN (also 2%), with the level position at 0.4 eV.

Substitutional Zn and Mg atoms on a cation site form shallow acceptor states. They are the most commonly used acceptors in the III nitrides. Our calculated level position for the Zn_{Ga} impurity in GaN is 0.3 eV above the VBM for the neutral state, and Zn_{Al} produces in AlN a level 0.4 eV above the VBM. Magnesium creates even shallower acceptor states. For both the Mg and the Zn impurities, we find outward relaxations. The shift is small in GaN, 4% and 2% of the bond length for Mg and Zn, respectively, but larger in AlN, 7% and 10%.

The pressure coefficients of defect levels are positive for all the dopants considered. They are small for shallow acceptor levels and large for donor levels lying close to the CBM.

IV. FORMATION ENERGIES

In Tables IV–VI the calculated formation energies of the defects considered are quoted. Only the neutral configurations are treated so that there is no dependency on the position of the Fermi level with respect to the band gap. The formation energy is defined with respect to the chemical potentials of the constituents, which depend on whether the nitride is grown under nitrogen-rich or -poor conditions (usually, experimental growth conditions are nitrogen-rich). Under cation-rich conditions, the cations are assumed in ther-

TABLE V. Calculated formation energies, in eV, for native defects and substitutional carbon, magnesium and zinc impurities in AlN. Also listed are the chemical potentials of the atoms, likewise in eV. Both Al-rich and N-rich growth conditions are considered. The calculated formation energy of bulk AlN is 3.9 eV.

	Al-rich	N-rich
μ_{Al}	−4.2	−8.1
μ_N	−12.2	−8.3
μ_C	−10.1	−10.1
μ_{Mg}	−1.7	−3.2
μ_{Zn}	−1.8	−1.8
V_{Al}	9.5	5.6
V_N	2.7	6.6
Al_N	9.7	17.5
N_{Al}	13.6	5.8
Mg_{Al}	2.5	0.16
Zn_{Al}	7.7	3.8
C_{Al}	8.6	4.7
C_N	1.9	5.8

modynamic equilibrium with its bulk solid phase, so that the chemical potentials are fixed at their bulk values, μ_B^{bulk}, μ_{Al}^{bulk}, or μ_{Ga}^{bulk}, while the nitrogen chemical potential is fixed by the growth condition:

$$\mu_B + \mu_N = \mu_{BN}^{bulk}, \quad \text{etc.} \tag{1}$$

Under nitrogen-rich conditions, the nitrogen in the nitride crystal is assumed to be in equilibrium with N_2 gas, so that $\mu_N = \mu_N^{gas}$, and the chemical potential of the cation is then fixed by the condition (1). The chemical potentials thus calculated are also quoted in the tables, in all cases given with respect to the free atom as given in the LDA (without atomic spin-polarization energy). The formation energies of the pure nitride crystals are given by

TABLE VI. Calculated formation energies, in eV, for native defects and substitutional carbon, magnesium and zinc impurities in GaN. Also listed are the chemical potentials of the atoms, likewise in eV. Both Ga-rich and N-rich growth conditions are considered. The calculated formation energy for bulk GaN is 1.9 eV.

	Ga-rich	N-rich
μ_{Ga}	−3.5	−5.5
μ_N	−10.2	−8.3
μ_C	−10.1	−10.1
μ_{Mg}	−1.7	−3.2
μ_{Zn}	−1.8	−1.8
V_{Ga}	8.2	6.3
V_N	2.7	4.6
Ga_N	6.7	10.5
N_{Ga}	9.7	5.8
Mg_{Ga}	1.0	0.6
Zn_{Ga}	2.4	0.5
C_{Ga}	6.5	4.6
C_N	2.6	4.5

$$E_{BN}^f = \mu_{BN}^{bulk} - \mu_B^{bulk} - \mu_N^{gas}, \quad \text{etc.} \tag{2}$$

The calculated values are $E_{BN}^f = 3.9$ eV, $E_{AlN}^f = 3.9$ eV, and $E_{GaN}^f = 1.9$ eV, respectively, which can be compared to the experimental values of 2.67 eV, 3.21 eV, and 1.23 eV.[23,24] The calculated formation energies are 20–50% larger than the experimental values, which reflects the tendency of the LDA to overestimate cohesion. For the impurity atoms C, Zn, and Mg, we use the bulk phase as reference for the impurity formation energy, with the exception of Mg under nitrogen-rich conditions, which we (following Ref. 25) assume to be bound in Mg_3N_2 molecules. The calculated impurity formation energies in Tables IV–VI are therefore all purely calculated LDA values, and none of the numbers depend on free atomic energies. In view of the general uncertainty of LDA mentioned above, the numbers cannot be regarded as very accurate, and we will focus here on trends.

For BN grown under N-rich conditions, the boron vacancy V_B is seen to have a low formation energy of 4.5 eV for the neutral configuration. Since V_B is a triple acceptor with the acceptor levels in the lower half of the band gap, this means that for n-type material, V_B will in fact be present in the $3-$ charge state, and the formation energy will be lower than that of the neutral state by the contribution

$$\Delta E(V_B) = 3E_F - \epsilon(0/-) - \epsilon(-/--) - \epsilon(--/3-), \tag{3}$$

where E_F is the Fermi level, and the ϵ's are the acceptor levels. Consequently, for E_F larger than ~ 3.2 eV, or midgap, the V_B formation energy becomes negative, and this defect becomes abundant in large numbers.

The neutral N_B defect has a formation energy of 6.0 eV, but in this case we find rather shallow donor levels, which for $\epsilon(0/-)$ is ~ 1 eV below the conduction-band edge, i.e., for highly *n*-type material, the N_B defect formation energy may be lowered by 1 eV for the first electron occupying this state and possibly by a fraction of an eV for the next electron, in the N_B^{--} defect, the level of which most probably will be very shallow. Thus we are led to conclude that N_B is not likely to be created in great abundance in *n*-type BN grown under N-rich conditions. On the other hand, in p-type BN grown under N-rich conditions, the V_N^+ defect may have a very low formation energy, as the single electron in the p-like gap state becomes ionized. The B_N antisite has a large formation energy under N-rich growth, and even with two low-lying acceptor levels, this defect is not likely to be created.

The C_B defect has a low formation energy, 3.3 eV, in the neutral state and will become favorable in *p*-type material, when the shallow donor level is depopulated. The formation energy of C_N is somewhat higher, 5.9 eV, but due to its shallow acceptor level, it will become negatively charged in *n*-type BN with an energy gain close to the value of the gap of 6 eV.

For BN grown under B-rich conditions, we notice that the B_N^{--} and C_N^- defects will have a negative formation energy in *n*-type material, and the V_N^+ likewise in *p*-type material, while the other defects are unlikely to be created.

For the native defects in AlN, we find that V_{Al} has a low formation energy of 5.6 eV when grown under N-rich con-

ditions, and as for V_B in BN, this defect has a sequence of acceptor levels in the lower half of the band gap, which will render the formation energy of the V_{Al}^{3-} defect stable in n-type material. The N_{Al} defect has a formation energy of 5.8 eV, similar to the N antisite in BN. The acceptor levels lie lower in the band gap for N_{Al}, which will make this defect more abundant in n-type AlN than the N_B in n-type BN. The V_N and Al_N defects have too large formation energies to be of any relevance in AlN grown under N-rich conditions.

For Mg_{Al} the very low formation energy will render this defect stable under almost any conditions. Zn_{Al} with a formation energy of 3.8 eV will have a negative formation energy in the negative charge state for n-type material.

For substitutional C impurities in AlN, grown under N-rich conditions, the formation energies are calculated to be 4.7 and 5.8 eV for C_{Al} and C_N, respectively. According to our calculations, relaxations of the N neighbors to the C_{Al} defect cause an electron to be donated to the Fermi level (the a_1 gap state moves into the conduction band, cf. Table II), which means that the formation energy of C_{Al}^+ in p-type material is lowered essentially by the band-gap energy, i.e., the formation energy turns negative. Therefore, C impurity atoms should easily be incorporated as C_{Al}^+ defects. In contrast, C_N yields a shallow acceptor level that will render C_N^- the preferred C defect in n-type material.

Under Al-rich growth conditions, only the V_N, Mg_{Al}, and C_N are calculated to have sufficiently low formation energy to be of any relevance in AlN. The V_N^+ defect is likely to be very abundant in p-type material, while Mg_{Al}^- and C_N^- will have negative formation energies in n-type AlN.

In GaN the energetics of the native defects are similar to the case of AlN. The V_{Ga}^{3-} will again be abundant in n-type GaN grown under N-rich conditions, while N_{Ga}^{--} is less likely to be created due to the smaller band gap of GaN of 3.3 eV. In p-type GaN grown under Ga-rich conditions, the V_N^+ defect will dominate. The results also show that excess Ga is most easily incorporated by the formation of N vacancies, similar to the result for AlN—but in that case the Al atom is so large that the Al_N antisite is unlikely as a defect. Mg and Zn impurity atoms readily replace Ga under any condition. Substitutional C in GaN behaves similarly to the case where AlN is the host, i.e., the C_{Ga}^+ defect will be most likely in p-type material grown under N-rich conditions, while C_N^- will be most likely in n-type material grown under Ga-rich conditions.

V. DISCUSSION AND SUMMARY

In conclusion, we have calculated in cubic GaN, AlN, and BN the electronic structure and formation energies of native defects and some common dopants, discussing the lattice relaxation and pressure effects. Several theoretical papers have been discussing native defects and impurity atoms in GaN and AlN.[5,25–31,4,19,8] In Refs. 26–29, and 8, the V_N^+ and V_{Ga}^{3-} were concluded to be the dominating native defects in GaN, similar to the conclusions of the present work, although some numerical details are different. In AlN similar importance of the vacancies was concluded,[28,8,25] in addition to the interstitial Al in p-type AlN.[25] Si, O, Mg, and C have been found to be the most abundant impurity atoms in GaN,[26,32,8] while the same impurity atoms with exception of C are abundant in AlN.[32,8,25]

The present calculations predict similar trends in the positions of defect levels in GaN, AlN, and BN, but the absolute values are different mainly due to the different values of the energy gaps. Generally, the defect levels are lying somewhat deeper in the energy gap in AlN and BN than in GaN. In particular, some states that are resonant with the conduction or valence band in GaN (as V_N) have in AlN and BN moved into the band gap.

The supercell calculations show pronounced outward lattice relaxations around cation antisites. In the more complex case of the nitrogen antisite, which seems to be similar in GaN and AlN to the EL2 in GaAs, large inward relaxation is found. The distance from the N impurity atom to the nearest neighbor is reduced by $\approx 30\%$ and becomes comparable to the N_2 dimer bond length. The above effect does not occur in BN; instead we observe outward, symmetrical relaxation of the surrounding atoms (about 9%). A pronounced inward relaxation (about 18% of the bond length) is found also around the C impurity on the cation site in GaN and in AlN, whereas, in BN, the relaxations around a C impurity is small or negligible. Substantial outward relaxations are found also for Mg and Zn impurities in AlN.

We notice, that outward relaxations in general are larger in AlN than in GaN, maybe because the Ga-3d electrons prevent the Ga-N bond length from becoming too short.[21] Where comparisons can be made, our results are similar to those obtained by means of first-principles pseudopotential calculations.[16,18,19,22,21,26] In BN relaxations are generally smaller (except for the boron vacancy), which can be due to the similar values of the atomic covalent radii of B, N, and C.

We have shown that, in all nitrides considered here, the pressure coefficients of the defect states depend on the position of the state in the gap, and they do not depend on the type of state, i.e., whether they are donors or acceptors. The pressure coefficients of the energy gaps at the Γ point are very similar in GaN and AlN (around 40 meV/GPa) and decidedly smaller in BN (14 meV/GPa). Also, the absolute values of the pressure coefficients of the defect states in GaN and AlN are similar and smaller in BN. Concerning the pressure behavior we can group all the defect states into three categories:

(1) States degenerate with the VBM and up to 0.5 eV (in BN up to 1 eV) for neutral, or up to 2 eV above the VBM for charged states. They are V_{cat}, C_N, Mg_{cat}, Zn_{cat}, and s-like state of V_N. The pressure coefficients of these defect energy levels are very small, positive or negative (from -5 meV/GPa to 4 meV/GPa).

(2) States lying close to the middle of the energy gap. Here are all antisites (except boron antisite). The pressure coefficients of these states are between 9 and 23 meV/GPa.

(3) States degenerate with the CBM or just below. (V_N, C_{cat}). The pressure coefficients are between 12 and 37 meV/GPa (in BN between 5 and 14 meV/GPa).

In evaluating these results one should bear in mind that the defect levels are given with respect to the VBM. States close to the band edges follow these, as one would expect. Comparing to existing experimental data, we find good agreement of the pressure coefficients of the Mg and Zn

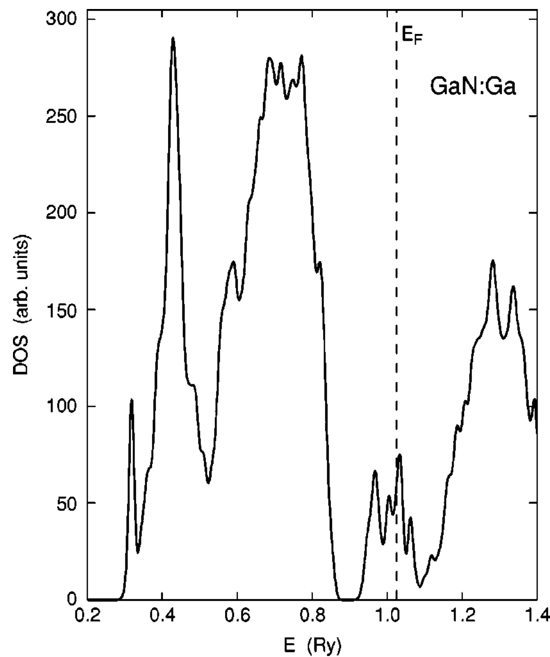

FIG. 3. The total density of states for the case of a neutral Ga antisite in GaN, calculated in a 32-atom supercell. The dashed line marks the Fermi level, which intersects the impurity band in proportion 4:2.

originated defect states; their pressure dependence is practically the same as the pressure behavior of the maximum of the valence band.[32]

As already pointed out, the supercell calculations lead to impurity bands with finite width, and we can only estimate the impurity level position as the center of gravity of the impurity band. This was determined by means of the density-of-states functions. For illustration, let us consider the case of the gallium antisite in GaN. The charge occupation of the p-like defect state is four electrons, and the Fermi energy is located in the impurity band dividing it in the ratio: 4:2 (4 occupied, 2 empty states). This situation is seen in Fig. 3, where the total density of states is presented. Much simpler is the case of a half-occupied state (cation vacancies and carbon at cation site) where the Fermi level is located in the center of the impurity band. Then the only difficulty is to find a good reference energy (VBM or CBM). This, however, is not straightforward due to the deformations of the valence and conduction bands caused by the defect. The most difficult cases in this context are the states, which are located close to the CBM (as nitrogen vacancy and C on cation site), and consequently their calculated energies seem to be less reliable than others. Also comparison with the GF calculations for these states is difficult because resonant states or states lying very close to the VBM or the CBM cannot be calculated by the present GF approach.

The energy levels as quoted in this paper are the eigenvalues of the self-consistent Kohn-Sham equations. A comparison to experiments in fact should rather be made by using calculated transition-state energies (i.e., using half-integer occupation numbers). Often a good approximation to this is obtained by averaging eigenvalues for ''neighboring'' charge states.[33,34]

ACKNOWLEDGMENT

This work was partially supported by KBN (Polish Science Committee) Grant No. 3P03B 093 14, by Grant No. 9600998 from the Danish Natural Science Research Council, and by the Danish Rector's Conference.

*Permanent address: High Pressure Research Center PAN, Sokolowska 29, 01-142 Warsaw, Poland.

[1] For review, see, *Semiconductors and Semimetals*, edited by J.I. Pankove and T.D. Moustakas (Academic Press, New York, 1997), Vol. 50; S. Nakamura and G. Fasol, *Blue Laser Diode* (Springer-Verlag, Berlin, 1997).
[2] C.H. Park and D.J. Chadi, Phys. Rev. B **55**, 12 995 (1997).
[3] P. Boguslawski and J. Bernholc, Phys. Rev. B **56**, 9496 (1997).
[4] J. Neugebauer and C. G. van de Walle, Appl. Phys. Lett. **69**, 503 (1996).
[5] C. G. van de Walle, Phys. Rev. B **57**, R2033 (1998).
[6] Y. Okamoto, M. Saito, and A. Oshiyama, Jpn. J. Appl. Phys., Part 2 **35**, L807 (1996).
[7] Chris Van de Walle, Phys. Rev. B **56**, R10 020 (1997).
[8] T. Mattila and R. M. Nieminen, Phys. Rev. B **55**, 9571 (1997).
[9] R.H. Wentorf, J. Chem. Phys. **26**, 956 (1957).
[10] R.M. Chrenko, Solid State Commun. **14**, 511 (1974).
[11] I. Gorczyca, N.E. Christensen, and A. Svane, Solid State Commun. **101**, 747 (1997).
[12] O. Gunnarsson, O. Jepsen, and O. K. Andersen, Phys. Rev. B **27**, 7144 (1983).
[13] O.K. Andersen, Phys. Rev. B **12**, 3060 (1975).
[14] M. Methfessel, Phys. Rev. B **38**, 1537 (1988).
[15] R. O. Jones and O. Gunnarsson, Rev. Mod. Phys. **61**, 681 (1989).
[16] J. Neugebauer and C. G. Van de Walle, Phys. Rev. B **50**, 8067 (1994).
[17] N.E. Christensen and I. Gorczyca, Phys. Rev. B **50**, 4397 (1994).
[18] P. Boguslawski, E. L. Briggs, and J. Bernholc, Phys. Rev. B **51**, 17 255 (1995).
[19] T. Mattila, A.P. Seitsonen, and R.M. Nieminen, Phys. Rev. B **54**, 1474 (1996).
[20] A. Zunger and A. Katzir, Phys. Rev. B **11**, 2378 (1975).
[21] J. Neugebauer and C. G. van de Walle, in *Diamond, SiC and Nitride Wide Bandgap Semiconductors*, edited by C. H. Carter, Jr., G. Gildenblat, S. Nakamura, and R. J. Nemamich, MRS Symposia Proceedings No. 339 (Materials Research Society, Pittsburgh, 1994), p. 687.
[22] P. Boguslawski and J. Bernholc, Acta Phys. Pol. A **90**, 735 (1996).
[23] W. A. Harrison, *Electronic Structure and the Properties of Solids* (Freeman, San Fransisco, 1980).
[24] C. Kittel, *Solid State Physics*, 5th ed. (Wiley, New York, 1976).
[25] C. Stampfl and C. G. van de Walle, Appl. Phys. Lett. **72**, 459 (1998).
[26] J. Neugebauer and C. G. van de Walle, in *Materials Theory, Simulations, and Parallel Algorithms*, edited by E. Kaxiras, J. Joannopoulos, P. Vashishta, and R. K. Kalia, MRS Symposia Proceedings No. 408 (Materials Research Society, Pittsburgh, 1996), p. 43.
[27] J. Neugebauer and C. G. van de Walle, Phys. Rev. B **50**, 8067 (1994).
[28] P. Boguslawski, E. Briggs, T. A. White, M. G. Wensell, and J. Bernholc (Ref. 21), p. 693.

[29] P. Boguslawski, E.L. Briggs, and J. Bernholc, Phys. Rev. B **51**, 17 255 (1995).
[30] T. Mattila, R. M. Nieminen, and A.P. Seitsonen, in *III-V Nitride Materials and Processes*, edited by T. D. Moustakas, J. P. Dismukes, and S. J. Pearton, (Electrochemical Society, Pennington, 1996), p. 205.
[31] T. Mattila and R. M. Nieminen, Phys. Rev. B **54**, 16 676 (1996).
[32] H. Teisseyre, T. Suski, P. Perlin, I. Gorczyca, M. Leszczynski, I. Grzegory, and S. Porowski, Mater. Sci. Forum **196**, 43 (1995).
[33] J. C. Slater, *Quantum Theory of Molecules and Solids* (McGraw-Hill, New York, 1974), Vol. IV.
[34] J.F. Janak, Phys. Rev. B **18**, 7165 (1978).